

Growth of Ge Thick Layers on Si(001) Substrates Using Reduced Pressure Chemical Vapor Deposition

Ji-Soo PARK, Michael CURTIN, Jie BAI, Mark CARROLL and Anthony LOCHTEFELD

AmberWave Systems Corp., 13 Garabedian Drive, Salem, NH 03079, U.S.A.

(Received July 12, 2006; accepted September 3, 2006; published online November 8, 2006)

Growth of Ge thick layers with and without a low temperature Ge buffer has been investigated using reduced pressure chemical vapor deposition with emphasis on the evolution of surface morphology and its roughness. Growth at 400 °C exhibited a 200 s incubation period for which about 1 equivalent monolayer of Ge was deposited with a surface roughness of around 0.1 nm followed by an abrupt increase due to an island growth. Higher growth temperature resulted in shorter or no observed incubation period and led to rougher surface due to larger size of islands. Ge layers grown at 600 °C on at low temperature Ge buffer first grown at 400 °C exhibited around 1 nm surface roughness independent of the layer thickness, which is much lower than those at 400–600 °C without the low temperature buffer. The Ge thick layer with the low temperature Ge buffer had thinner defective interface of Ge/Si than that without the buffer.

[DOI: [10.1143/JJAP.45.8581](https://doi.org/10.1143/JJAP.45.8581)]

KEYWORDS: germanium, chemical vapor deposition, buffer, surface morphology, island growth

1. Introduction

The growth of Ge thick layers on Si(001) has been of considerable interest due to the importance of applications such as efficient photodetectors operating in the low absorption regions (1.3–1.55 μm wavelength) of silica fibers,^{1,2)} optical interconnects,^{3,4)} Si-based optoelectronics integrated circuits,⁵⁾ and Ge-based transistors.⁶⁾ One of the greatest challenges in Ge heteroepitaxy on Si is high surface roughness due to island growth. Lattice mismatch of 4.2% between Ge and Si causes a transition from initial, pseudomorphic, two-dimensional (2D) wetting layers to three-dimensional (3D) islands for the relaxation of misfit strain.⁷⁾

For the growth of Ge thick layers with low surface roughness, a thin Ge buffer at low temperatures (330–450 °C) followed by a high temperature (600–850 °C) growth for Ge thick layer has been proposed.⁸⁾ A low temperature Ge buffer of 30–50 nm thickness enables plastic relaxation and an additional thicker Ge layer is grown at high temperature for higher crystalline quality and growth rate.^{8–12)} Ge growth on a SiGe buffer with a Ge concentration gradient,^{13,14)} which leads to several micrometer-thick buffers, has been widely used, but it is not appropriate for the applications requiring lower thickness of 300–400 nm. Colace *et al.*⁸⁾ reported that Ge thick layers with low surface roughness were grown at 600 °C after 50-nm-thick Ge buffer at 330 °C using ultrahigh vacuum chemical vapor deposition (UHV-CVD) and near-infrared photodetectors were fabricated on the layers. Luan *et al.*¹⁰⁾ demonstrated high quality Ge epilayers on Si with low threading-dislocation densities using two-step UHV-CVD and cyclic thermal annealing. Hartmann *et al.*¹¹⁾ also reported flat and thick Ge layers on Si using a low temperature Ge buffer grown at 400 °C in a reduced pressure CVD (RP-CVD). However, there have been few studies on how 3D island growth of Ge on Si can affect the surface morphology and roughness of Ge thick layers with and without low temperature Ge buffers.

In present research, the evolution of surface morphology of Ge layers on Si and its effect on surface roughness of Ge thick layers have been investigated using a standard

production RP-CVD system. A comparison was made between with and without a low temperature Ge buffer and incubation period and surface roughness at different growth temperatures were also discussed.

2. Experimental Details

Ge layers were grown on p-type Si(001) substrates of ~0.02 Ω cm resistivity and 200 mm diameter in an industrial ASM Epsilon E2000 system, which is a horizontal, cold-wall, single wafer, load-locked reactor with a lamp-heated graphite susceptor in a quartz tube. Si substrates were cleaned in a diluted HF solution and rinsed in DI water followed by an *in-situ* bake at 870 °C and at the same pressure for the growth for 1 min in H₂ prior to growth. 20 slm hydrogen and 30 sccm germane (GeH₄) diluted at 25% in H₂ were flowing as a carrier gas and the source gas of Ge, respectively. Growth temperature was varied from 400 to 600 °C and pressure was fixed at 80 Torr. For two-step growth, a 55-nm-thick Ge buffer was first grown at 400 °C for 540 s and then a thick Ge layer was grown at 600 °C. The samples were characterized using tapping-mode atomic force microscopy (AFM; Veeco Dimension 3000) and transmission electron microscopy (TEM; JEOL JEM 2100). The amount (i.e., areal density) of Ge deposited was measured by Rutherford backscattering spectrometry and expressed in equivalent monolayers (eq-MLs) of Ge (1 eq-ML of Ge = 6.3×10^{14} atoms/cm²). Scanning electron microscopy and grazing incidence X-ray reflectivity spectra were used to measure the thickness of Ge layers.

3. Results

Figure 1(a) shows thickness of Ge layers deposited at 400 °C as a function of growth time. Ge thickness was linearly increased with growth time (i.e., constant growth rate) and there was a significant incubation time of about 200 s. Ge layers grown in two-step at 600 °C as the second step showed a constant growth rate of 0.58 nm/s up to 1200 s as shown in Fig. 1(b).

Surface morphology of Ge layers grown at different temperatures for different growth times was characterized using AFM. Figure 2 shows the surface images of Ge layers grown at 400 °C for different growth times. For 90 s growth

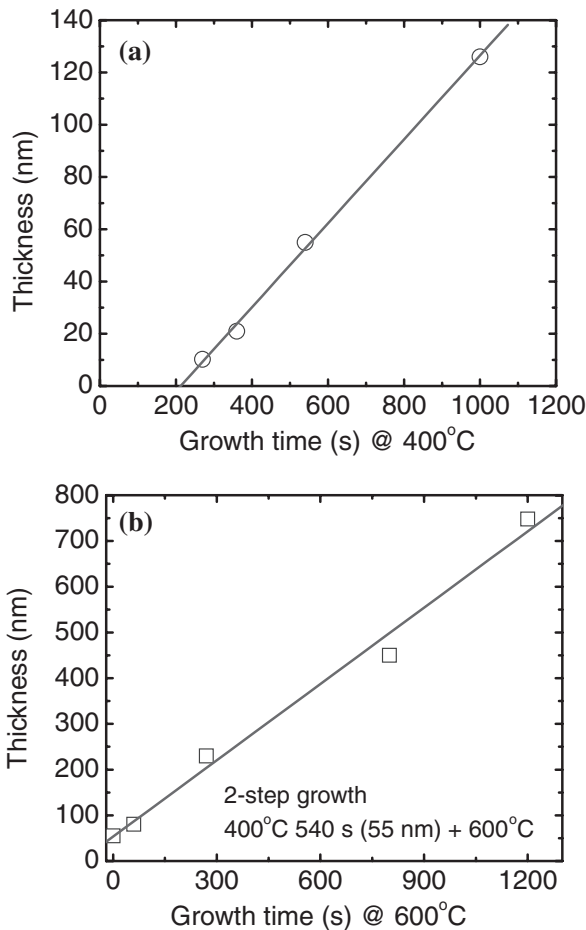


Fig. 1. Thickness of Ge layers deposited (a) at 400 and (b) at 600 °C on the low temperature buffer at 400 °C as a function of growth time.

[Fig. 2(a)], the nucleated Ge which is less than 0.5 eq-ML exhibited an alignment along $\langle 110 \rangle$. At 120 s, very tiny islands which also aligned along $\langle 110 \rangle$ were observed and some islands were about to grow larger as indicated by arrow in Fig. 2(b). When 1 eq-ML of Ge was deposited after 180 s growth, sharp and tiny islands were formed [Fig. 2(c)], but rms roughness was still as low as 0.11 nm. Further Ge deposition beyond 1 eq-ML led to an abrupt change of the surface; rms roughness of 70.5 eq-MLs of Ge after 270 s growth was increased to 4.46 nm which was caused by the formation of clustered 3D islands and their partial coalescence [Fig. 2(d)] and they got bigger as the growth continued [Fig. 2(e)].

Ge growth at 500 °C showed more serious island growth than that at 400 °C as shown in Fig. 3. With 2.3 eq-MLs of Ge after 10 s growth, the surface was covered with sharp and tiny islands [Fig. 3(a)], and its surface microstructure is basically similar with that of the Ge layer grown at 400 °C for 180 s [Fig. 2(c)] although the island density at 500 °C was much higher. The same trend was found after the growth of the islands as the 400 °C growth; an abrupt increase of surface roughness caused by discrete 3D islands [Fig. 3(b)]. 2D surface images (not shown here) more clearly shows that they are hut clusters, which were reported to be faceted square pyramids or elongated pyramids bound by $\{105\}$ planes.¹⁵⁾ With increasing growth time, the hut clusters became larger [Fig. 3(c)] and then more rounded (“domes”)

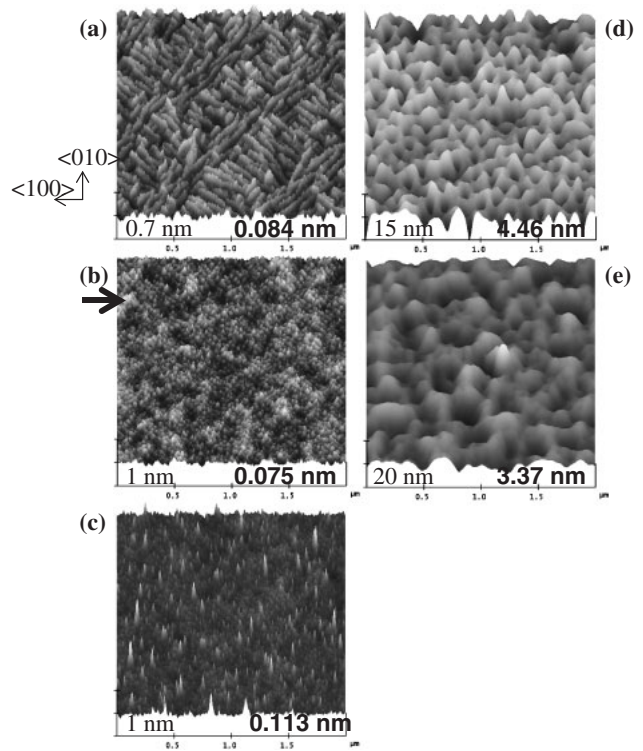


Fig. 2. AFM images of Ge layers deposited at 400 °C for (a) 90 s, (b) 120 s, (c) 180 s (1 eq-ML), (d) 270 s (71 eq-MLs), and (e) 360 s. Scan size is $2 \times 2 \mu\text{m}^2$. Vertical scale and rms roughness is shown on the left and right bottom of each image, respectively.

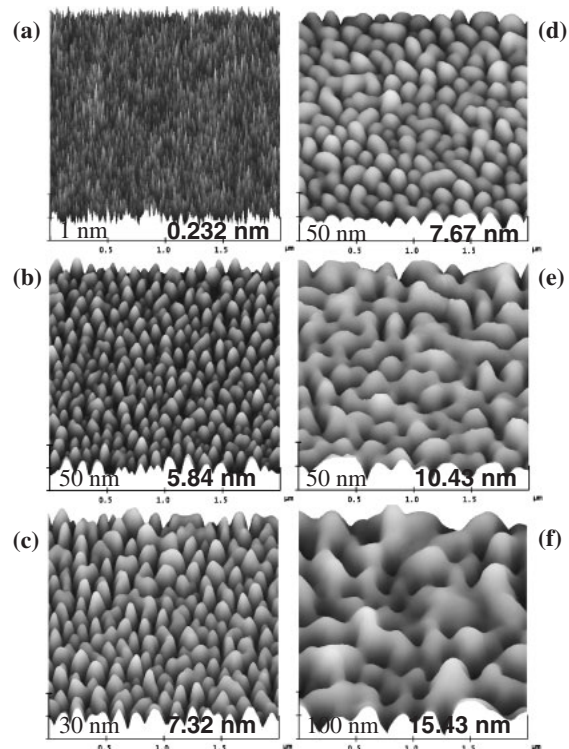


Fig. 3. AFM images of Ge layers deposited at 500 °C for (a) 10 s (2.3 eq-MLs), (b) 30 s, (c) 60 s, (d) 90 s, (e) 180 s, and (f) 270 s. Scan size is $2 \times 2 \mu\text{m}^2$. Vertical scale and rms roughness is shown on the left and right bottom of each image, respectively.

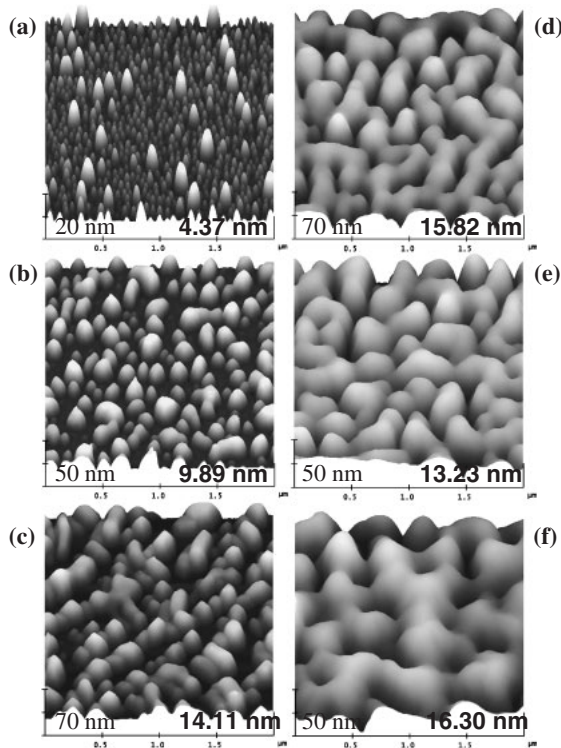


Fig. 4. AFM images of Ge layers deposited at 600°C for (a) 5 s (15 eq-MLs), (b) 15 s (42 eq-MLs), (c) 30 s, (d) 60 s, (e) 90 s, and (f) 180 s. Scan size is $2 \times 2 \mu\text{m}^2$. Vertical scale and rms roughness is shown on the left and right bottom of each image, respectively.

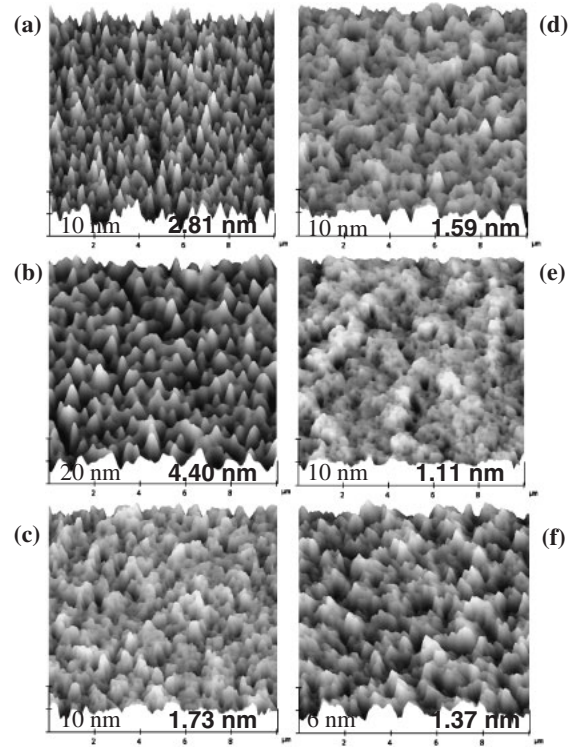


Fig. 5. AFM images of Ge layers deposited at 400°C for (a) 540 s, (b) 1000 s in one-step, and at 600°C for (c) 60 s, (d) 90 s, (e) 180 s, and (f) 270 s on the low temperature buffer at 400°C. Scan size is $10 \times 10 \mu\text{m}^2$. Vertical scale and rms roughness is shown on the left and right bottom of each image, respectively.

with even larger size [Fig. 3(d)]. And they are coalesced one another [Fig. 3(e)] which is quite similar with the layer grown for 270 s at 400°C in Fig. 2(d) although Ge islands at 500°C was larger than those at 400°C. And they became even larger as the growth continued resulting in much rougher surface of Ge layer [Fig. 3(f)].

At 600°C, 14.9 eq-MLs of Ge were deposited and its surface roughness was already over 4 nm after as short as 5 sec growth [Fig. 4(a)]. The size of small islands was fairly uniform except some larger islands, which is consistent with a bimodal distribution of Ge islands grown at similar temperature and low pressure.^{16,17} As the growth proceeded, the islands got larger and rounded with their density lower [Fig. 4(b), 41.9 eq-MLs of Ge], began to be partially coalesced [Fig. 4(c)], and were connected one another followed by getting even larger causing rougher surface [Figs. 4(d)–4(f)]. This is also similar with the growth at 400°C [Figs. 2(d) and 2(e)] and 500°C [Figs. 3(e) and 3(f)] but higher growth temperature led to larger islands and rougher surface.

Surface morphology of Ge layers grown in two-step was compared in Fig. 5. Figures 5(a) and 5(b) are surface images of Ge layers grown at 400°C for 540 and 1000 s, respectively. Longer growth time caused rougher surface due to the larger size of islands, but its surface microstructure was not changed much over the growth time; partially coalesced large 3D islands. However, Ge layers grown at 600°C as the second step on the buffers first grown at 400°C for 540 s showed different surface microstructure as shown in Figs. 5(c)–5(f) compared to the ones in Fig. 5(b). A further second step growth showed lower

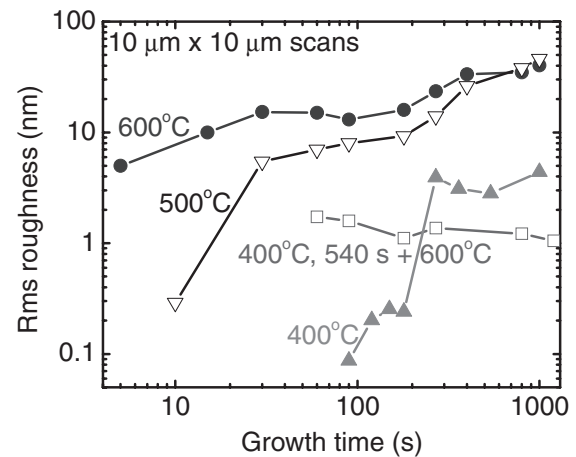


Fig. 6. Rms roughness values of Ge layers grown at 400, 500, and 600°C without the buffer and at 600°C on the low temperature buffer grown at 400°C as a function of growth time. The roughness values were obtained from AFM images of $10 \times 10 \mu\text{m}^2$ scan size.

surface roughness around 1 nm unlike the growth at 400–600°C without the buffer.

Rms roughness values of the Ge layers grown at 400–600°C with and without the the low temperature buffer at 400°C were plotted as a function of growth time in Fig. 6. Ge layers grown at 400°C had less than 1 nm roughness up to 200 s, but over 200 s its roughness was abruptly increased to about 4 nm and 2–4 nm roughness values were kept to 1000 s. At 500°C, roughness was increased from 0.3 nm to around 4 nm after 10 s growth, continued to increase as the

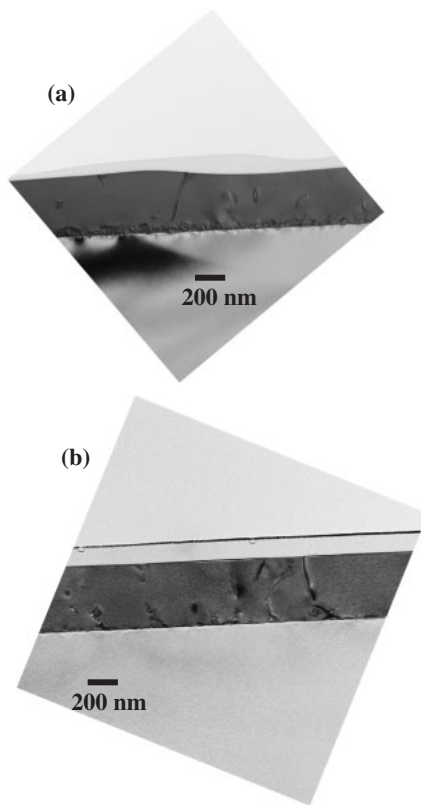


Fig. 7. Cross-sectional TEM images of Ge layers (a) grown at 600 °C for 1000 s without the low temperature buffer and (b) at 600 °C for 800 s on the low temperature buffer.

growth proceeded and reached about 50 nm after 1000 s growth. The 600 °C growth showed a similar trend but its surface roughness was already 5 nm after as short as 5 s and reached about 40 nm after 1000 s growth. In contrast, Ge layers grown on the low temperature buffer showed fairly constant surface roughness between 1 and 2 nm even after 1200 s growth at 600 °C.

Figures 7(a) and 7(b) show cross-sectional TEM images of Ge layers grown at 600 °C for 1000 s without the buffer and at 600 °C for 800 s on the low temperature buffer, respectively. The thickness of Ge layer grown without the buffer was not uniform compared to that with the buffer. In addition, the Ge layer without the buffer had a defective region around Ge/Si interface about 50 nm, whereas the one with the buffer grown in two-step exhibited thinner defective region.

4. Discussion

Ge growth at 400 °C exhibited an incubation time of about 200 s followed by a linear increase of thickness as a function of growth time with a constant growth rate of 0.16 nm/s obtained from the slope of Fig. 1(a). During the incubation period, Ge amounted about 1 eq-ML and growth rates evolved very slowly and surface roughness was as low as around 0.1 nm [Figs. 2(a)–2(c)]. But, after the incubation period, the surface roughness abruptly increased as 3D island growth started (Fig. 6). In addition, higher growth temperature resulted in shorter or no observed incubation period; Ge growth at 500 °C exhibited an abrupt increase of surface roughness from around 0.2 nm to over 5 nm after 10 s

(2.3 eq-MLs) growth [Figs. 3(a) and 3(b), and 6], which shows basically similar surface microstructure of sharp and tiny islands at 400 °C just before the end of incubation period [Fig. 2(c)]. And an incubation period was not observed at 600 °C; 15 eq-MLs of Ge were deposited and its roughness was already over 4 nm after 5 s growth. The incubation period at low temperature and low pressure is consistent with previous reports. Kamins *et al.*¹⁸⁾ reported that a 30 s incubation time was observed followed by a constant growth rate at 550 °C at reduced pressure of 10 Torr, but no incubation time was found at higher pressure which led to higher growth rate. And Halbax *et al.*¹²⁾ also showed that Ge layers grown at 330 °C in UHV-CVD showed a constant growth rate after 15 min incubation time. Kobayashi *et al.*¹⁹⁾ reported that a 12 min incubation period was observed at 350 °C and at 75 mTorr only when hydrogen gas was used as a carrier gas and lower growth pressure resulted in longer incubation time. Since Ge atoms do not completely cover the Si surface during the incubation period, the observed slow growth rate during the period should be mainly related to Ge growth from germane on Si(001) surface.¹²⁾ Once the Si surface is covered by Ge over 1 eq-ML, Ge is grown on Ge surface leading to a constant growth rate and rougher surface due to 3D island growth. But, the increased growth rate at higher temperature or pressure can make an incubation period shorter by quicker Ge coverage of Si substrates. Also, it was reported that when Ar was used as a carrier gas in Ge growth, a drastic reduction of an incubation period was observed compared with the case of hydrogen, which was believed to be caused by the suppression of adsorption and/or decomposition of germane on the H-terminated Si surface in the case of hydrogen.¹⁹⁾ And atomic hydrogen was reported to be act as a surfactant suppressing island formation of Ge on Si substrates at low temperature.^{20,21)} Thus, the incubation period at low temperature might be also related to the presence of hydrogen during growth.

Regarding the evolution of Ge islands, it was generally reported that after deposition of a wetting layer of a few MLs, small clusters of faceted square pyramids or elongated rectangular pyramids (huts) bounded by {105} planes appear.^{16–18,22)} Larger islands with more rounded and multi-faceted features (domes) are formed at later stages.^{16–18,22)} If the growth continues, very large islands with diameter of several hundred nm appear and dislocations are created inside the islands.^{22,23)} At 400 °C, due to a long incubation period and low growth rate, surface features up to 1 eq-ML is well observed [Figs. 2(a)–2(c)]. But, after the incubation period, the Ge surface has coalesced clusters of huts and domes [Fig. 2(d)] and this results in a quite large surface roughness of 2.8 nm on the 55-nm-thick buffer [Fig. 5(a)]. Thus, the growth temperature used to form a low temperature Ge buffer was not low enough to inhibit 3D island growth and faceting from occurring. However, growing a Ge thick layer at 600 °C was sufficient to obtain a fairly smooth surface with surface roughness around 1 nm independent of Ge layer thickness of over 700 nm (Fig. 6).

If Ge islands at 500 °C [Figs. 3(b)–3(d)] are compared with the ones at 600 °C [Figs. 4(a)–4(c)] before partially coalesced and connected one another, it is found that the density of Ge islands at 600 °C is reduced and their size

become larger quickly. The larger size of Ge islands with lower density causes much rougher surface with increasing growth time. This should result from faster surface diffusion at higher temperature at which Ge atoms are more likely to diffuse to existing islands rather than clustering to form a new nucleus. Smaller islands were reported to be formed when the amount of Ge and the growth temperature were reduced to prevent the system from reaching thermodynamic equilibrium.²⁴⁾ Or since Ge islands nucleate at strain-induced irregularities,²⁵⁾ the more thermal energy available for strain relaxation may possibly contribute to the lower density of nuclei at the higher temperature.¹⁸⁾

The Ge layers grown on the low temperature buffer had much lower surface roughness than without the buffer. Ge layers grown at 600 °C as the second step on the layers first grown at 400 °C exhibited different surface microstructure from those at 400–600 °C without the buffer. Interestingly, the former has lower surface roughness than the latter grown at 400 °C in spite of higher growth temperature in the second step (Figs. 5 and 6). Low temperature Ge layers show an inhibited 3D island growth reportedly due to a reduced surface diffusion of Ge atoms and hydrogen surfactant effect as discussed above. It was reported that in the first step of low temperature growth, Ge layers plastically relax the strain in the Ge layers with inhibiting 3D island growth and the second step of higher growth temperature allows lowering dislocation density and reducing overall deposition time similar to the homoepitaxial case.¹¹⁾ But, the reason of low surface roughness of the Ge layers grown at higher growth temperature in the second step is not clear at this time and is under further investigation.

Cross-sectional TEM image of Ge layers grown at 600 °C in one-step exhibit that the Ge layer grown without the buffer has thicker defective region of 50 nm than the one grown in two-step (Fig. 7). Kim *et al.*²⁶⁾ showed that a single Ge island was formed in pattern dimensions less than 420 nm. LeGoues *et al.*²⁷⁾ observed in TEM the formation of an edge dislocation network in molecular beam epitaxy Ge on Si within 8 eq-MLs of deposition. Langdo *et al.*²⁸⁾ showed that Ge layer grown in nanoholes had much thinner defective interface region than that on unpatterned Si due to small number of islands was formed in the nanohole. From these results, the thicker defective region at the interface might be related to the growth of 3D islands and their coalescence. Considering that lower temperature Ge growth gave rise to more inhibited 3D island growth, it is conjectured that the formation of 3D Ge islands at higher temperature and their coalescence during growth might cause more interactions between dislocations causing thicker defective interface.

5. Conclusions

Ge growth at 400 °C exhibited 200 s incubation time for which about 1 eq-ML was deposited with surface roughness of low as around 0.1 nm followed by an abrupt increase due to 3D island growth. Higher growth temperature resulted in shorter or no observed incubation period resulting from higher growth rate and reduced hydrogen surfactant effect. Also, it led to rougher surface due to larger size of islands. The Ge layers in two-step on the first grown 400 °C Ge buffers showed lower surface roughness than those grown at

400 °C in one-step independent of the layer thickness. The Ge layer with the buffer had thinner defective region at Ge/Si interface than the one without the buffer, which might be caused by the 3D island growth and their coalescence and more interactions between dislocations.

Acknowledgements

The authors acknowledge Daniel Tseng of Evans Analytical group for RBS and Michelle Stawasz of ATMI for AFM analysis.

- 1) G. Masini, L. Colace and G. Assanto: *Mater. Sci. Eng. B* **89** (2001) 2.
- 2) R. Calaraco, M. Fiordelisi, S. Lagomarsino and F. Scarinci: *Thin Solid Films* **391** (2001) 138.
- 3) S. Lardenois, D. Pascal, L. Vivien, E. Cassan, S. Laval, R. Orobitchouk, M. Heitzmann, N. Bouzaida and L. Mollard: *Opt. Lett.* **28** (2003) 1150.
- 4) K. K. Lee, D. R. Lim, L. C. Kimerling, J. Shin and F. Cerrina: *Opt. Lett.* **26** (2001) 1988.
- 5) L. M. Giovane, D. R. Lim, S. H. Ahn, T. D. Chen, J. S. Foresi, L. Liao, E. J. Oulette, A. M. Agarwal, X. Duan, J. Michel, A. Thilderkvist and L. C. Kimerling: *Mater. Res. Soc. Symp. Proc.* **486** (1998) 45.
- 6) W. P. Bai, N. Lu, A. Ritenour, M. L. Lee, D. A. Antoniadis and D.-L. Kwong: *IEEE Electron Device Lett.* **27** (2006) 175.
- 7) D. J. Eaglesham and M. Cerullo: *Phys. Rev. Lett.* **64** (1990) 1943.
- 8) L. Colace, G. Masini, F. Galluzzi, G. Assanto, G. Capellini, L. Di Gaspare, E. Palange and F. Evangelisti: *Appl. Phys. Lett.* **72** (1998) 3175.
- 9) S. Fama, L. Colace, G. Masini, G. Assanto and H.-C. Luan: *Appl. Phys. Lett.* **81** (2002) 586.
- 10) H.-C. Luan, R. R. Lim, K. K. Lee, K. M. Chen, J. S. Sandland, K. Wada and L. C. Kimerling: *Appl. Phys. Lett.* **75** (1999) 2909.
- 11) J. M. Hartmann, A. Abbadie, A. m. Papon, P. Holliger, G. Rolland, T. Billon, J. M. Fedeli, M. Rouviere, L. Vivien and S. Laval: *J. Appl. Phys.* **95** (2004) 5905.
- 12) M. Halbwx, D. Bouchier, V. Yam, D. Debarre, L. H. Nguyen, Y. Zheng, P. Rosner, M. Benamara, H. P. Strunk and C. Clerc: *J. Appl. Phys.* **97** (2005) 064907.
- 13) M. T. Currie, S. B. Samavedam, T. A. Langdo, C. W. Leitz and E. A. Fitzgerald: *Appl. Phys. Lett.* **72** (1998) 1718.
- 14) R. Calaraco, M. Fiordelisi, S. Lagomarsino and F. Scarinci: *Thin Solid Films* **391** (2001) 138.
- 15) Y.-W. Mo, D. E. Savage, B. S. Swartzentruber and M. G. Lagally: *Phys. Rev. Lett.* **65** (1990) 1020.
- 16) M. Goryll, L. Vescan and H. Luth: *Mater. Sci. Eng. B* **69–70** (2000) 251.
- 17) T. I. Kamins, G. Medeiros-Ribeiro, D. A. A. Ohlberg and R. S. Williams: *J. Appl. Phys.* **94** (2003) 4215.
- 18) T. I. Kamins, E. C. Carr, R. S. Williams and S. J. Rosner: *J. Appl. Phys.* **81** (1997) 211.
- 19) S. Kobayashi, M. Sakuraba, T. Matsuura, J. Murota and N. Mikoshiba: *J. Cryst. Growth* **174** (1997) 686.
- 20) A. Sakasi and T. Tatsumi: *Appl. Phys. Lett.* **64** (1994) 52.
- 21) D. J. Eaglesham, F. C. Unterwand and D. C. Jacobson: *Phys. Rev. Lett.* **70** (1993) 966.
- 22) S. A. Chaparro, Y. Zhang, J. Druvker, D. Chandrasekhar and D. J. Smith: *J. Appl. Phys.* **87** (2000) 2245.
- 23) M. Goryll, L. Vescan and H. Luth: *Thin Solid Films* **336** (1998) 244.
- 24) M. Goryll, L. Vescan, K. Schmidt, S. Mesters, H. Luth and K. Szot: *Appl. Phys. Lett.* **71** (1997) 410.
- 25) V. Yam, Vinh Le Thanh, P. Boucaud, D. Debarre and D. Bouchier: *J. Vac. Sci. Technol. B* **20** (2002) 1251.
- 26) E. Kim, N. Usami and Y. Shiraki: *Semicond. Sci. Technol.* **14** (1999) 257.
- 27) F. K. LeGoues, M. Copel and R. Trom: *Phys. Rev. Lett.* **63** (1989) 1826.
- 28) T. A. Langdo, C. W. Leitz, M. T. Currie, E. A. Fitzgerald, A. Lochtefeld and D. A. Antoniadis: *Appl. Phys. Lett.* **76** (2000) 3700.